charge-transfer reaction in an approximate, albeit more straightforward, fashion.

The solvent-induced deviations from the TST rate have been shown to track the relative rate of charge transfer;[5] i.e., the solvent modification to the barrier is electrostatic in nature. These deviations are not strongly influenced by the relatively small geometrical changes of the solute but are strongly dependent on the rapidly shifting solute charge in the transition-state region. The latter occurs with quite small solute geometry changes. Therefore, we can obtain a good estimate of κ if we neglect the explicit dependence of U_{uv} on solute geometry changes but retain the parametric dependence of the potential. The use of this approach has obvious advantages in the present context, since the spatial solute–solvent distribution functions evaluated for a solute with the transition-state geometry are readily accessible. To use the present results, we then simply evaluate the derivative appearing in the last term in eq 15 via the *parametric* dependence of the coupling constants appearing in U_{uv} on r_A and then evaluate the average over the solvent distribution characterizing the transition state. This last step is completely analogous to the evaluation of the average potential energy and can be done by using the solute–solvent site–site correlation functions evaluated from the integral equation for the transition-state geometry ($r_A = 0$).

When applied to our system (μ = 18.214 amu; see ref 18), we find the values $\omega_b = (k_b/\mu)^{1/2}$ = 376.1 cm^{-1}, $\omega_{b,eq}$ = 542.9 cm^{-1}, and

$$\langle d^2U_{uv}/dr_A^2\rangle_{S,r_A=0} = 10.06 \text{ kcal/(mol Å}^2)$$

Equation 16 then predicts a correction factor κ = 0.59, in reasonable accord with the value derived from the lengthy simulation studies[5] of 0.55.

The very close comparison should be viewed as in part fortuitous since the models used are somewhat different. Our barrier is apparently somewhat broader, and our solvent somewhat more polar, so that κ might be expected to be somewhat smaller for our system than for that simulated. At the same time, our neglect of explicit geometric dependence should lead to systematic overestimation of κ; the simulated result with no charge transfer yields κ = 0.9, while we would obtain essentially κ = 1. Nevertheless, the general agreement (both values roughly one-half) indicates that the approach is a useful and efficient one for processes dominated by the charge-transfer aspect.

IV. Conclusions

We have carried out a detailed study of the gas-phase energy and solvated, free energy surfaces for the reaction of chloride with methyl chloride in water, focusing on behavior in the transition-state region. By employing the extended RISM integral equation to treat the solvation, we have examined the free energy surface at a level of detail that is not easily accessible via simulation with its associated statistical error. Correspondingly, the energy and entropy components are readily separable here. The variation of behavior with solvent polarity has also been efficiently examined, and the tendency for saturation behavior in the activation free energy for polarities as high as that of water has been demonstrated. Using this surface and the nonadiabatic solvation theory of Hynes and co-workers, we have shown that for the limiting case of fast reaction and rapid charge transfer, the corrections to transition-state theory due to solvent fluctuations are readily calculable from the integral equation results.

The present calculations have demonstrated the importance of properly describing the variation of the interatomic potentials in the transition-state region if a physically meaningful free energy surface in this region is desired.

The integral equation method provides a valuable complement to the methods of computer simulation, providing rapid access to qualitatively reliable descriptions of reaction free energy surfaces. Application of these methods to a wider range of reactions and solvents appears very worthwhile.

Acknowledgment. Support of this work by a grant from the National Institute of General Medical Sciences is gratefully acknowledged, as is computational support from the University of Texas System Center for High Performance Computing. P.J.R. is the recipient of an NSF Presidential Young Investigator Award and a Camille and Henry Dreyfus Foundation Teacher-Scholar Award.

Registry No. CH_3Cl, 74-87-3; Cl, 16887-00-6.

Reassignment of the Structure of $Si(CO)_2$ Based on Theoretically Predicted IR Spectra

Roger S. Grev* and Henry F. Schaefer, III

Contribution CCQC No. 46 from the Center for Computational Quantum Chemistry, School of Chemical Sciences, University of Georgia, Athens, Georgia 30602. *Received January 3, 1989*

Abstract: Self-consistent-field methods show that the lowest energy structure of $Si(CO)_2$ is a strongly bent C_{2v} symmetry structure more akin to that of a transition-metal carbonyl than to its isovalent quasi-linear first-row analogue carbon suboxide. Configuration interaction predictions of isotopic shifts in C–O stretching vibrational frequencies for this isomer agree with those previously observed experimentally, as do the differences in C–O frequencies between the mono- and dicarbonyl. Thus, we suggest a reassignment of the observed spectra from that of the previously assumed $D_{\infty h}$ structure to the C_{2v} symmetry $^1A_1$ state found here.

Hypothesis

In a pioneering study on the reaction of silicon atoms with typical main-group ligands, Lembke, Ferrante, and Weltner (LFW) found[1] that silicon could add either one or two carbon monoxide molecules to form SiCO and $Si(CO)_2$, but only one of the isoelectronic nitrogen molecules would add, forming SiN_2. This was in perfect agreement with reactions of carbon atoms and CO and N_2 ligands where, once again, no compound of the form N_2CN_2 was in evidence, but CCO, $C(CO)_2$, and CNN were easily formed.

Confirmation of the formation of the dicarbonyl, $Si(CO)_2$, was provided by the appearance of the (seemingly) proper number of infrared C–O stretching vibrational frequencies after annealing

(1) Lembke, R. R.; Ferrante, R. F.; Weltner, W., Jr. *J. Am. Chem. Soc.* **1977**, *99*, 416.

0002-7863/89/1511-5687$01.50/0

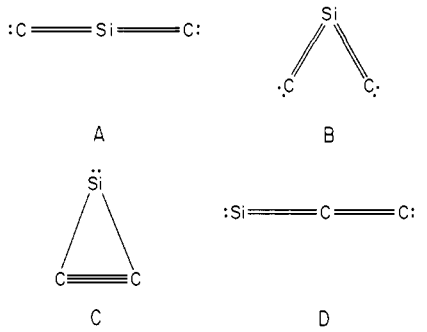

Figure 1. Qualitative valence structures for the SiC_2 molecule.

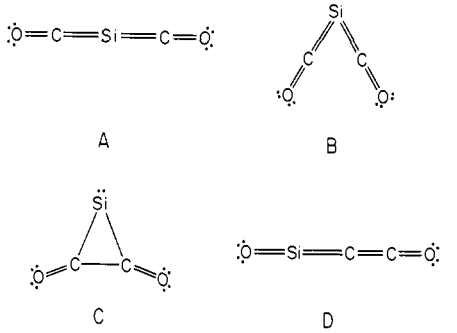

Figure 2. Qualitative valence structures for the SiC_2O_2 molecule.

a matrix of isotopically substituted SiCO. Specifically, the two strong IR bands at 1899.3 and 1855.3 cm^{-1} attributed to $Si^{12}CO$ and $Si^{13}CO$ were replaced by three bands at 1928, 1899.6, and 1886 cm^{-1} and were assigned to the IR active C-O stretching fundamentals of the (assumed) centrosymmetric $O^{12}CSi^{12}CO$, $O^{12}CSi^{13}CO$, and $O^{13}CSi^{13}CO$ molecules, respectively. Similar observations were made for $^{12}C-^{16}O$ and $^{12}C-^{18}O$ mixtures.

The assumption by LFW of a linear $D_{\infty h}$ structure for $Si(CO)_2$ was by analogy with the molecule $C(CO)_2$, carbon suboxide, which is an extensively studied quasi-linear molecule O=C=C=C=O.[2] The minimum energy geometry of C_3O_2 is thought to be bent by about 20°, with a very small barrier to linearity (near 30 cm^{-1}), making it effectively linear. In this respect C_3O_2 is similar to many other molecules that contain a cumulene (C=C=C) linkage such as propadienone (H_2C=C=C=O),[3] propadienethione (H_2C=C=C=S),[4] and carbon subsulfide (S=C=C=C=S)[2], all of which are either quasi-linear or have very low C-C-C bending frequencies. Indeed this characteristic is shared by the C_3 molecule itself, which has a bending frequency[5-7] of only 63 cm^{-1}. In this sense, the C_3 portion of carbon suboxide may be considered the "structure making" part of the above molecules.

At the time of their study (1976), LFW's assumption that $Si(CO)_2$ would be similar, structurally, to $C(CO)_2$ was entirely reasonable, as the first multiply bonded silicon compounds had not yet been characterized. In the 1980s, however, a wealth of data has accumulated to show that *unsaturated* heavier main-group compounds often differ substantially from their first-row counterparts, and the greater the degree of unsaturation, the less similar the structures. As an example H_2Si=SiH_2 is much like ethylene although it is slightly trans bent, but HSi≡SiH is not at all like acetylene and adopts, instead, a minimum energy structure with dibridged hydrogens.[8] Thus we should not be surprised if the highly unsaturated structure O=C=Si=C=O is not the minimum energy conformer as LFW assumed.

Of even greater, and more direct, significance is the fact that the possible structure making part of an OCSiCO molecule, i.e., the CSiC fragment, is not even remotely analogous to C_3.[9,10] For instance C=Si=C is not a minimum at linear geometries but instead, upon reducing the symmetry to C_{2v}, adopts a highly bent structure with a C-Si-C angle around 60° that lies about 50 kcal/mol below linear CSiC (Figure 1B). The global minimum on the SiC_2 surface is an even more strongly bent ring structure (Figure 1C), which lies approximately 135 kcal/mol below linear CSiC. Also low lying, though not likely to be important in the reactions of silicon atoms with carbon monoxide, is the linear SiCC structure (Figure 1D). This was long believed to be the ground state of SiC_2 until combined theoretical/experimental studies in the early 1980s proved that structure C of Figure 1 was in fact the ground state,[9,10] with the linear SiCC isomer from 1-5 kcal/mol higher lying.

Considering, then, the strong structural similarities between the C_3 molecule and the related propadienone, propadienethione, carbon subsulfide, and carbon suboxide molecules and assuming that similar analogies will hold between CSiC and OCSiCO, we might predict that structures like those seen in parts B-D of Figure 2 are low-lying isomers of SiC_2O_2 but that a linear OCSiCO isomer (Figure 2A) might not correspond to a minimum on the potential energy surface and in any event would be very high-lying.

To test these simple predictions and to ascertain the structure of the $Si(CO)_2$ isomer observed by LFW, we have engaged in an ab initio theoretical study of the SiC_2O_2 potential surface. By a direct comparison of experimentally observed and theoretically predicted C-O vibrational frequencies for the various isotopomers, we will show that the species observed by LFW was most likely of the general form in Figure 2B.

Theoretical Methods

Geometrical structures corresponding to the valence isomers of Figure 2 have been precisely determined at the self-consistent-field (SCF) level of theory by employing analytic gradient techniques.[11,12] Standard Huzinaga-Dunning[13-15] basis sets of double-ζ (DZ) quality, technically designated Si(11s7p/6s4p); C,O(9s5p/4s2p), to which a single set of Cartesian d functions has been appended (DZP), are used throughout. The d function exponents are $\alpha_d(Si) = 0.5$, $\alpha_d(C) = 0.75$, and $\alpha_d(O) = 0.85$. Analytic SCF second-derivative methods[16] are used to determine the harmonic vibrational frequencies and, therefore, the nature (i.e., minima, transition state, etc.) of the various stationary points, and analytic determination of dipole moment derivatives was employed for the evaluation of infrared intensities.[17]

The two lowest lying isomers (Figure 2B,D) have been reoptimized at the SCF level using a larger triple-ζ (TZ) valence basis set to which two sets of d functions with $\alpha_d(Si) = 1.0, 0.25$, and $\alpha_d(C,O) = 1.5, 0.35$ have been added (TZ2P). The s-p set for silicon is McLean and Chander's 6s5p contraction[18] of Huzinaga's 12s9p primitive set, and for carbon and oxygen it is Dunning's 5s3p contraction[14] of Huzinaga's 9s5p set used above.

The effects of electron correlation on the relative energies of the various isomers have been determined by the method of configuration

(2) See the review by: Winnewisser, B. P. In *Molecular Spectroscopy: Modern Research*; Rao, K. N., Ed.; Academic Press: Orlando, FL, 1985; Vol. 3, pp 321-419, and references therein.
(3) Brown, R. D.; Godfrey, P. D.; Champion, R. *J. Mol. Spectrosc.* **1987**, *123*, 93.
(4) Brown, R. D.; Dyall, K. G.; Elmes, P. S.; Godfrey, P. D.; McNaughton, D. *J. Am. Chem. Soc.* **1988**, *110*, 789.
(5) Douglas, A. E. *Astrophys. J.* **1951**, *114*, 466.
(6) Gausset, L.; Herzberg, G.; Lagerqvist, A.; Rosen, A. *Astrophys. J.* **1965**, *142*, 45.
(7) Liskow, D. H.; Bender, C. F.; Schaefer, H. F. *J. Chem. Phys.* **1972**, *56*, 5075.
(8) See, e.g.: Gordon M. S. In *Molecular Structures and Energetics*; Liebman, J. F., Greenberg A., Eds.; Springer-Verlag: New York, 1986; Vol. 1, pp 101-122, and references therein.
(9) Grev, R. S.; Schaefer, H. F. *J. Chem. Phys.* **1984**, *80*, 3552.
(10) Michalopoulos, D. L.; Geusic, M. E.; Langridge-Smith, P. R. R.; Smalley, R. E. *J. Chem. Phys.* **1984**, *80*, 3556.
(11) Pulay, P. *Modern Theoretical Chemistry*; Schaefer, H. F., Ed.; Plenum: New York, 1977; Vol. 4 pp 153-183.
(12) Dupuis, M.; King, H. F. *J. Chem. Phys.* **1978**, *68*, 3998.
(13) Huzinaga, S. *J. Chem. Phys.* **1965**, *42*, 1293.
(14) Dunning, T. H. *J. Chem. Phys.* **1970**, *53*, 2823.
(15) Dunning, T. H.; Hay, P. J. *Modern Theoretical Chemistry*; Schaefer, H. F., Ed.; Plenum: New York, 1977; Vol. 3, pp 1-27.
(16) Saxe, P.; Yamaguchi, Y.; Schaefer, H. F. *J. Chem. Phys.* **1982**, *77*, 5647.
(17) Yamaguchi, Y.; Frisch, M.; Gaw, J.; Schaefer, H. F.; Binkley, J. S. *J. Chem. Phys.* **1986**, *84*, 2262.
(18) McLean, A. D.; Chandler, G. S. *J. Chem. Phys.* **1980**, *72*, 5639.

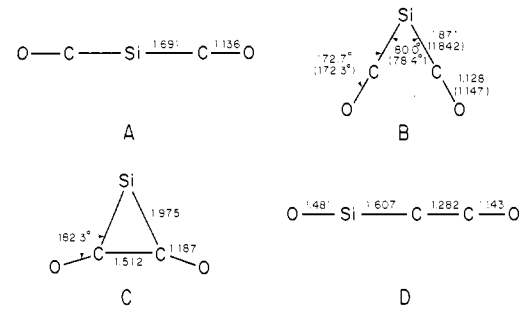

Figure 3. DZP SCF-optimized geometries for SiC_2O_2 corresponding to the valence structures of Figure 2. The DZP CISD-optimized geometry of isomer B is listed in parentheses. Distances are given in angstroms.

Table I. Total Energies (hartrees) and Relative Energies (Given in Parentheses in Units of kcal/mol) Obtained at Various Levels of Theory with a DZP Basis Set for the Structures in Figure 3

structure	SCF	CISD	CISD+Q
$^1\Sigma_g^+$ (A)	−514.21740 (89.8)	−514.80108 (80.5)	−514.89380 (76.7)
$^1A_1$ (B)	−514.36052 (0.0)	−514.92935 (0.0)	−515.01596 (0.0)
$^1A_1$ (C)	−514.25068 (68.9)	−514.82071 (68.2)	−514.90733 (68.2)
$^1\Sigma^+$ (D)	−514.35379 (4.2)	−514.92429 (3.2)	−515.00689 (5.7)

interaction (CI) in conjunction with the DZP basis set at the SCF-optimized geometry. The core orbitals and their virtual orbital counterparts have been frozen throughout, otherwise all single and double excitations with respect to the SCF reference have been included (CISD).[19] In the largest case (Figure 2D) this result in 66 331 configuration state functions (CSFs) when computed in C_{2v} symmetry. The effects of unlinked quadruple excitations have been estimated by the method of Davidson (CISD+Q).[20]

Since the only connection with experiment for $Si(CO)_2$ is a single C–O stretching frequency and its shift upon isotopic substitution, we found it necessary to reproduce the harmonic force field and associated vibrational frequencies of the lowest lying isomer (Figure 2B) at the highest level of theory possible. Thus, structure B in Figure 2 was reoptimized using the CISD wave function (63 713 CSFs) with the DZP basis set by analytic CI gradient techniques.[21] The harmonic vibrational frequencies and quadratic force constants were then determined via finite differences of analytic gradients along plus and minus distortions (0.01 Å or 0.02 rad) of symmetrized internal coordinates. This involves determination of the wave function and gradient including up to 127 057 CSFs in the case of b_2 symmetry displacements into the C_s subgroup of C_{2v}. The infrared intensities were determined by finite difference methods as well, with dipole moments evaluated as energy derivatives.

Structures and Energies

The DZP SCF-optimized geometries of the valence structures in Figure 2 are shown in Figure 3, and the corresponding total and relative energies (given in parentheses) are in Table I. For comparison, we note the following prototypical single- and multiple-bond distances obtained at similar levels of theory:[22-24] r(C=O) = 1.189 Å in H_2CO; r(C=O) = 1.117 Å in carbon monoxide; r(Si–C) = 1.889 Å in H_3SiCH_3; r(Si=C) = 1.692 Å in $H_2Si{=}CH_2$; r(C–C) = 1.534 Å in H_3CCH_3; r(C=C) = 1.315 Å in $H_2C{=}CH_2$; r(Si=O) = 1.494 Å in $H_2Si{=}O$.

As expected from the qualitative considerations in the Hypothesis, the linear $^1\Sigma_g^+$ state of $Si(CO)_2$ (Figure 3A) is not a minimum on the potential energy surface. Examination of its harmonic vibrational frequencies shows an imaginary degenerate π_u mode, $\omega(\pi_u) = 541i$ cm^{-1}, which leads, upon optimization within the C_{2v} subgroup of $D_{\infty h}$, to a $^1A_1$ state with the structure B in Figure 3. This is exactly analogous to the case of the linear C=Si=C molecule mentioned earlier. This $^1A_1$ structure is a local minimum on the $Si(CO)_2$ surface and lies 76.7 kcal/mol below the linear $^1\Sigma_g^+$ state at the CISD+Q level of theory. The Si–C bond distance of 1.871 Å in the $^1A_1$ state is only slightly shorter than a normal Si–C single bond, and the C–O bond distance is 0.01 Å longer than in free C–O. Thus the correspondence between the valence electron structure in Figure 2B (which incorporates two Si=C bonds) and the geometry in Figure 3B is not a very good one. The Si–C and C–O bond distances are, however, nearly identical with those found at the same level of theory in $^3\Sigma^-$ SiCO (r(Si–C) = 1.876 Å and r(C–O) = 1.127 Å), which may be profitably considered as a silicon ^3P atom with a CO ligand coordinately bonded to it.[25] In a similar way, then, we might prefer to think of structure B in Figure 3 as a ^1D silicon atom with two coordinately bonded carbonyl groups. Specifically, if the molecule is in the y–z plane, then taking the silicon atom valence electrons to be in a $s^2p_x^2$ configuration correctly predicts both the total symmetry orbital occupations and the fact that the two highest lying MO's are essentially silicon 3s and $3p_x$ in character.

The other C_{2v} symmetry $^1A_1$ state, structure C of Figure 3, is also a local minimum, but it lies 68 kcal/mol higher than structure B in Figure 3. Apparently the three-membered ring leads to significant destabilization of Figure 3C. In the case of Figure 1C the ring strain is compensated by the formation of additional C–C bonds compared to parts B or D of Figure 1, but here the strain is aggravated by the loss of the stronger C–O π bonds. Except for an abnormally long Si–C distance, the optimized geometry in Figure 3C is easily related to its valence electron structure C in Figure 2.

The final structure considered here (Figure 3D) is also a minimum at the DZP SCF level of theory. This result must be cautiously interpreted, however, as numerous other cumulene-type structures are known to exhibit subtle geometry/basis set dependencies. For example :C=C=C: is found to be a linear minimum with a DZ basis set, but bent with DZP, and linear once again with a TZP basis set.[7] Similarly, :Si=C=Si: is a linear minimum with DZP but significantly bent when a second set of polarization functions are added to the basis set.[26] Too, O=C=C=C=O displays a sensitive geometric dependence on the nature of the basis set.[27] For these reasons, the O=Si=C=C=O isomer's geometry has also been reoptimized at the SCF level with the TZ2P basis set. The resultant parameters (r(O–Si) 1.477; r(Si–C) = 1.607; r(C–C) = 1.274; r(C–O) = 1.130 Å), are not significantly different from the DZP ones, but the structure is now found *not* to be a minimum. Instead, it has a degenerate imaginary frequency $\nu(\pi) = 51i$ cm^{-1}, which leads to the kinked structure found in Figure 4, a scant 0.10 kcal/mol below the linear $^1\Sigma$ structure.

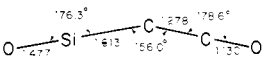

Figure 4. TZ2P SCF C_s symmetry optimized geometry corresponding to isomer D in Figure 3.

We should note that this intriguing result has led us to reinvestigate the linear Si=C=C isomer itself. This molecule has been the subject of numerous studies[28-30] since the discovery[9,10] that it is *not* the ground state of SiC_2, mostly with an eye toward its eventual characterization as a very low-lying stable isomer. Preliminary results employing correlated wave functions with large basis sets indicate that the linear SiCC isomer might not exist as a stable minimum on the SiC_2 potential energy surface.

(19) Saxe, P.; Fox, D. J.; Schaefer, H. F.; Handy, N. C. *J. Chem. Phys.* **1982**, *77*, 5584.
(20) Langhoff, S. R.; Davidson, E. R. *Int. J. Quantum Chem.* **1974**, *8*, 61.
(21) (a) Brooks, B. R.; Laidig, W. D.; Saxe, P.; Goddard, J. D.; Yamaguchi, Y.; Schaefer, H. F. *J. Chem. Phys.* **1980**, *72*, 4652. (b) Rice, J. E.; Amos, R. D.; Handy, N. C.; Lee, T. J.; Schaefer, H. F. *J. Chem. Phys.* **1986**, *85*, 963.
(22) Scuseria, G. E.; Schaefer, H. F. *J. Chem. Phys.* **1989**, *90*, 3629.
(23) Schmidt, M. W.; Truong, P. N.; Gordon, M. S. *J. Am. Chem. Soc.* **1987**, *109*, 5217.
(24) Yoshioka, Y.; Schaefer, H. F. *J. Am. Chem. Soc.* **1981**, *103*, 7366.
(25) DeKock, R. L.; Grev, R. S.; Schaefer, H. F. *J. Chem. Phys.* **1988**, *89*, 3016.
(26) Grev, R. S.; Schaefer, H. F. *J. Chem. Phys.* **1985**, *82*, 4126.
(27) Amos, R. D. *Chem. Phys. Lett.* **1984**, *108*, 347.
(28) Pauzat, F.; Ellinger, Y. *Chem. Phys. Lett.* **1984**, *112*, 519.
(29) Oddershede, J.; Sabin, J. R.; Diercksen, G. H. F.; Grüner, N. E. *J. Chem. Phys.* **1985**, *83*, 1702.
(30) Sadlej, A. J.; Diercksen, G. H. F.; Oddershede, J.; Sabin, J. R. *Chem. Phys.* **1988**, *122*, 297.

Table II. Harmonic Vibrational Frequencies (cm^{-1}) and Infrared Intensities (km/mol in Parentheses) of $Si(CO)_2$ in Figure 3B at the Self-Consistent-Field (SCF) and Configuration Interaction with All Single- and Double-Excitation (CISD) Levels of Theory with a DZP Basis Set

	SCF	CISD		SCF	CISD
ω_1 (a_1)	2328 (732)	2202 (586)	ω_6 (b_1)	408 (4.0)	387 (0.7)
ω_2 (a_1)	658 (20.4)	663 (20.6)	ω_7 (b_2)	2207 (1985)	2087 (1646)
ω_3 (a_1)	488 (7.8)	512 (15.2)	ω_8 (b_2)	477 (63.1)	538 (37.3)
ω_4 (a_1)	124 (3.1)	117 (2.8)	ω_9 (b_2)	392 (8.7)	391 (10.3)
ω_5 (a_2)	461 (0.0)	450 (0.0)			

Table III. Harmonic Vibrational Frequency ω_7 for the Various Isotopic Mass Combinations of OCSiCO in the $^1A_1$ State of Figure 3B and Their Shifts Relative to the Principal Isomer (Given in Parentheses) at the SCF and CISD Levels of Theory

masses	SCF	CISD	expt[a]
16-12-28-12-16	2206.7	2087.2	1928
16-13-28-13-16	2158.2 (-48.5)	2040.2 (-47.0)	1886 (-42)
16-13-28-12-16	2177.3 (-29.4)	2058.6 (-28.6)	1899.6 (-28.4)
18-12-28-12-18	2152.5 (-54.2)	2037.7 (-49.5)	1882.5 (-45.5)
18-12-28-12-16	2173.8 (-32.9)	2057.2 (-30.0)	1897.5 (-30.5)

[a] Reference 1.

At the DZP SCF level of theory the $^1A_1$ state (Figure 3B) is 4.2 kcal/mol below Figure 3D. Single-point CISD energies decrease this value to 3.2 kcal/mol, but this increases to 5.7 kcal/mol at CISD+Q levels of theory. Given the small relative energy difference between these isomers and the qualitative (but not necessarily quantitative) change in the potential energy surface of the $^1\Sigma$ (or $^1A'$) state with the larger basis set, we have also reoptimized the geometry of Figure 3B with the TZ2P basis set. The geometry of the $^1A_1$ state changes only slightly to r(Si-C) = 1.871 Å, r(C-O) = 1.114 Å, θ(C-Si-C) = 79.8°, and θ(Si-C-O) = 173.4°. More importantly, the SCF energy difference between the $^1A_1$ state and the $^1A'$ state in Figure 4 increases to 5.8 kcal/mol, strongly suggesting that Figure 3B will remain the lower lying isomer.

Vibrational Frequencies of $Si(CO)_2$

While it is unlikely that the linear $^1\Sigma_g^+$ state of $Si(CO)_2$ assumed by LFW to be the ground state is the isomer observed in their matrix, it is not a priori obvious that the C_{2v} symmetry $^1A_1$ state we have found here is the species they observed either. Since the *only* experimental evidence for its existence is a single C-O stretching vibrational frequency and its shifts upon ^{13}C and ^{18}O isotopic substitution, we must take a close look at the predicted theoretical vibrational frequencies and isotopic shifts for this isomer to see if they match the experimental value.

The DZP SCF harmonic vibrational frequencies of structure B in Figure 3, and the associated infrared intensities, are given in Table II. The most intense mode, ω_7, at 2207 cm^{-1} appears in the expected range of 7-15% higher than the experimental value for the principal isotope of $Si(CO)_2$ observed at 1928 cm^{-1}. The other C-O stretching frequency, ω_1, has a significantly lower IR intensity and appears 121 cm^{-1} higher, so we may safely assume that ω_7 is the one that should correlate with the experimentally observed frequency *if* the $^1A_1$ state is the species observed by LFW.

The DZP SCF vibrational frequency predictions for ω_7 with the various isotopic mass conbinations of the OCSiCO framework, and their shifts (given in parentheses), are listed in Table III along with the experimental data obtained by LFW. Considering that the theoretically predicted values correspond to harmonic frequencies, whereas the experimental frequencies are anharmonic values, the overall agreement appears reasonable. The differences between the predicted and the observed frequency shifts at the SCF level are between 1 and 8.7 cm^{-1}. All in all, though, it is difficult to assess the absolute agreement with experiment. It simply is not obvious whether the match between the theoretical and the experimental shifts is sufficient to state that the molecule observed by LFW is, in fact, structure B of Figure 3.

There is one other quantity that we can compare with experiment, i.e., the difference between the CO stretching frequency of $^3\Sigma^-$ SiCO and the C-O stretching frequency in $Si(CO)_2$. Experimentally, the C-O stretch in $^3\Sigma^-$ SiCO is observed at 1899.3 cm^{-1} for the principal isomer, and this is replaced by a frequency at 1928 cm^{-1} after repeated warming–cooling cycles of the matrix. Thus, the frequency in $Si(CO)_2$ is 29 cm^{-1} *higher* than that in SiCO. In Table IV we list the values for ω_7 of $Si(CO)_2$ obtained in the present study along with the C-O stretching frequency of $^3\Sigma^-$ SiCO obtained in our previous investigation of the monoadducts.[25] Unlike the experiment, the DZP SCF stretching frequency is predicted to be 26 cm^{-1} *lower* in $Si(CO)_2$ than in SiCO.

Table IV. Comparison of ω_7 for the $^1A_1$ State of $Si(CO)_2$ in Figure 3B and the C-O Stretching Frequency in $^3\Sigma^-$ SiCO to the Experimentally Observed Values

	SCF	CISD	expt[a]
$Si(CO)_2$	2207	2087	1928
SiCO	2233[b]	2058[b]	1899.3
shift	-26	+29	+29

[a] Reference 1. [b] Reference 25.

Table V. Symmetry Coordinates for the $^1A_1$ State of Figure 3B[a]

species	coordinate
A_1	$S_1 = (2)^{-1/2}(R_1 + R_2)$
	$S_2 = (2)^{-1/2}(R_3 + R_4)$
	$S_3 = \Theta_1$
	$S_4 = (2)^{-1/2}(\Theta_2 + \Theta_3)$
A_2	$S_5 = \tau_1 + \tau_2$
B_1	$S_6 = \tau_1 - \tau_2$
B_2	$S_7 = (2)^{-1/2}(R_1 - R_2)$
	$S_8 = (2)^{-1/2}(R_3 - R_4)$
	$S_9 = (2)^{-1/2}(\Theta_2 - \Theta_3)$

[a] The simple internal coordinates are R_1 = Si-C_l; R_2 = Si-C_r; R_3 = C_l-O_l, R_4 = C_r-O_r; Θ_1 = C_l-Si-C_r; Θ_2 = Si-C_l-O_l; Θ_3 = Si-C_r-O_r; τ_1 = O_l-C_l-Si-C_r; τ_2 = O_r-C_r-Si-C_l where r and l refer to left and right.

Table VI. Theoretically Predicted Force Constants for the $^1A_1$ State of Figure 3B at the SCF and CISD Levels of Theory with the DZP Basis Set

species	constant	SCF	CISD
A_1	F_{11}	2.217	2.606
	F_{22}	21.992	19.490
	F_{33}	1.379	1.207
	F_{44}	0.485	0.477
	F_{12}	0.706	0.646
	F_{13}	0.253	0.231
	F_{14}	0.045	0.050
	F_{23}	0.392	0.399
	F_{24}	0.048	0.045
	F_{34}	0.264	0.253
A_2	F_{55}	0.009	0.009
B_1	F_{66}	0.007	0.007
B_2	F_{77}	2.016	2.620
	F_{88}	20.643	18.189
	F_{99}	0.400	0.399
	F_{78}	1.432	1.263
	F_{79}	0.007	-0.034
	F_{89}	-0.017	0.011

The lack of agreement between theory and experiment on the *sign* of the shift in the CO stretching frequency on going from SiCO to $Si(CO)_2$ convinced us to determine the geometry and vibrational frequencies of $Si(CO)_2$ at the CISD/DZP level of theory. The CISD/DZP-optimized geometry of the $^1A_1$ state of $Si(CO)_2$ is shown in parentheses in Figure 3B. The principal geometrical change at the correlated level is an increase in the C-O bond distance and a decrease in the Si-C bond distance. This is also reflected in the CISD vibrational frequencies shown in Table II, which are significantly shifted to lower values for the C-O stretches, but are largely unchanged or even slightly increased for the lower frequency modes involving Si-C stretches, or C-Si-C and Si-C-O bends.

The isotopic C-O stretching frequency shifts determined for ω_7 using the CISD wave function are also shown in Table III and are *universally* in better agreement with experiment than the SCF

results. The absolute differences between the theoretical harmonic frequency shifts and the anharmonic experimental shifts have been reduced to the 0.2-5.0 cm^{-1} range. That *all* of the frequency shifts come into better agreement with experiment as the theoretical model becomes more complete is almost as strong a statement about the $^1A_1$ state (Figure 3B) being the species observed by LFW as is the now overall good absolute agreement.

More convincing evidence that the spectra observed by LFW belongs to the $^1A_1$ state of Figure 3B is provided in Table IV, where we see that, at the CISD/DZP level of theory, the C-O stretching frequency, ω_7, in $Si(CO)_2$ is predicted to be 29 cm^{-1} *higher* than that in SiCO, in perfect agreement with experiment and in exact opposition to the SCF predictions.

Conclusion

Since it is so high-lying and does not correspond to a minimum on the potential energy surface, it seems clear that the linear centrosymmetric $^1\Sigma_g^+$ state of $Si(CO)_2$ is *not* the structure observed by Lembke, Ferrante, and Weltner[1] in their important matrix isolation studies. On the other hand, the agreement between the CISD theoretical predictions of the isotopic C-O frequency shifts and the experimentally observed values, coupled with the agreement between the theoretical and experimental C-O frequency differences between the SiCO and $Si(CO)_2$ molecules, provides strong evidence that the matrix IR spectra of LFW belongs to the $^1A_1$ state of C_{2v} symmetry in Figure 3B.

One important consequence of the proposed reduction in symmetry of the nuclear framework from $D_{\infty h}$ to C_{2v} is that the totally symmetric C-O stretching vibration, ω_1, is now IR active. At the CISD level of theory this mode is predicted to occur 115 cm^{-1} above the experimentally observed frequency ω_7, with about one-third the IR intensity. Predictions for the isotopic shifts corresponding to the mass combinations in Table III for this mode are 50.9, 20.4, 50.3, and 20.0 cm^{-1}, respectively. We hope these predictions will soon be verified in the laboratory. To aid the experimentalist, SCF and CISD force constants for structure B of Figure 3 are given in Table VI for the symmetry coordinates defined in Table V.

Finally, even though it seems likely that the experimentally observed spectra belong to the $^1A_1$ isomer in Figure 3B, there may well be lower lying isomers of SiC_2O_2. One intriguing possibility is a five-membered Si—O—C=C—O ring with 6π electrons. We leave these for possible future studies.

Acknowledgment. This research was supported by the U.S. National Science Foundation (Grant CHE-8718469).

Mono- and Bis(ethyne)nickel(0) Complexes

Klaus-Richard Pörschke

Contribution from the Max-Planck-Institut für Kohlenforschung, D-4330 Mülheim a.d. Ruhr, West Germany. *Received November 28, 1988*

Abstract: Various (ligand)nickel(0)-ethene complexes react with ethyne in ether or pentane at low temperature to afford crystalline compounds of types $(R_3P)_2Ni(C_2H_2)$, $\{(RO)_3P\}_2Ni(C_2H_2)$, $(^tBuNC)_2Ni(C_2H_2)$, $(R_3P)Ni(C_2H_2)(C_2H_4)$, $\{(R_3P)Ni(C_2H_4)\}_2(\mu\text{-}C_2H_2)$, $\{(R_3P)Ni(C_2H_2)\}_2(\mu\text{-}C_2H_2)$, and $(R_3P)Ni(C_2H_2)_2$ (R = Me, Et, ^{i}Pr, Ch, Ph). The chemical and spectroscopic properties of the new complexes are reported.

Several catalytic processes are known involving nickel and ethyne, including the Reppe carbonylation of ethyne to acrylic acid,[1a] the cyclooligomerization of ethyne, which forms cyclooctatetraene (cot),[2a] higher oligomers,[2b] and benzene and styrene,[2c] the dimerization of ethene by an $AlEt_3$/nickel(0) catalyst activated and modified by ethyne,[3] and cooligomerization reactions of butadiene and ethyne yielding various products.[4] Nevertheless, especially the mechanism of the impressive ethyne tetramerization reaction to afford cot is still in question despite continued efforts toward its elucidation.[5]

The first step of any catalytic reaction between nickel and ethyne should involve the coordination of an ethyne molecule to the nickel atom. Complexes of nickel with ethyne are known for oxidation states II, I, and 0. When nickel salts are dissolved in liquid ethyne at 25 °C under pressure, they form labile adducts $(C_2H_2)_nNiX_2$ (n = 1-3).[6a] Complexes $(bpy)Ni(^iC_4H_9)_2(C_2H_2)$ and $(Ph_3P)_2Ni(^iC_4H_9)_2(C_2H_2)$ are reported to result from the reaction of $Ni(acac)_2$ with $Al(^iC_4H_9)_3$ in the presence of the ligand molecules at -78 °C.[6b] From the reaction of Cp_2Ni with ethyne at 70 °C under pressure the dinuclear compound $(CpNi)_2(\mu\text{-}C_2H_2)$

Scheme I

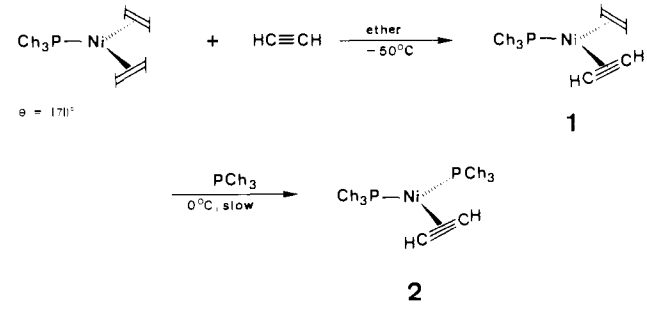

(1) Reppe, W. *Neue Entwicklungen auf dem Gebiet der Chemie des Acetylens und Kohlenoxids*; Springer: Berlin, 1949.

(2) (a) Reppe, W.; Schlichting, O.; Klager, K.; Toepel, T. *Liebigs Ann. Chem.* **1948**, *560*, 1. (b) Reppe, W.; Schlichting, O.; Meister, H. *Liebigs Ann. Chem.* **1948**, *560*, 93. (c) Reppe, W.; Schweckendiek, H. J. *Liebigs Ann. Chem.* **1948**, *560*, 104.

(3) (a) Ziegler, K.; Holzkamp, E.; Breil, H.; Martin, H. *Angew. Chem.* **1955**, *67*, 426, 541. Ziegler, K. *Brennst.-Chem.* **1954**, *35*, 321. (b) Ziegler, K.; Gellert, H.-G.; Holzkamp, E.; Wilke, G.; Duck, E. W.; Kroll, W.-R. *Liebigs Ann. Chem.* **1960**, *629*, 172.

(4) (a) Reed, H. W. B. *J. Chem. Soc.* **1954**, 1931. (b) Brenner, W.; Heimbach, P.; Wilke, G. *Liebigs Ann. Chem.* **1969**, *727*, 194. (c) Fahey, D. R. *J. Org. Chem.* **1972**, *37*, 4471.

(5) (a) Jolly, P. W.; Wilke, G. *The Organic Chemistry of Nickel*; Academic Press: New York, 1975; Vol. II, pp 94-132. (b) Jolly, P. W. In *Comprehensive Organometallic Chemistry*; Wilkinson, G., Stone, F. G. A., Abel, E. W., Eds.; Pergamon: London, 1982; Vol. 8, pp 649-670. For recent accounts see: (c) Colborn, R. E.; Vollhardt, K. P. C. *J. Am. Chem. Soc.* **1981**, *103*, 6259; **1986**, *108*, 5470. (d) Wilke, G. *Angew. Chem.* **1988**, *100*, 189; *Angew. Chem., Int. Ed. Engl.* **1988**, *27*, 185.

(6) (a) Tedeschi, R. J.; Moore, G. L. *Ind. Eng. Chem. Prod. Res. Dev.* **1970**, *9*, 83. (b) Chukhadzhyan, G. A.; Abramyan, Zh. I.; Grigoryan, V. G.; Avetisyan, D. V. *Arm. Khim. Zh.* **1970**, *23*, 860; *Chem. Abstr.* **1971**, *74*, 54206t. (c) Dubeck, M. U.S. Patent 3097224, 1963. Randall, E. W.; Rosenberg, E.; Milone, L.; Rosetti, R.; Stranghellini, P. L. *J. Organomet. Chem.* **1974**, *64*, 271. Wang, Y.; Coppens, P. *Inorg. Chem.* **1976**, *15*, 1122. (d) Ozin, G. A.; McIntosh, D. F.; Power, W. J.; Messmer, R. P. *Inorg. Chem.* **1981**, *20*, 1782.

0002-7863/89/1511-5691$01.50/0